metals

Article

Production of Closed-Cell Foams Out of Aluminum Chip Waste: Mathematical Modeling and Optimization

Jure Krolo , Branimir Lela *, Karla Grgić and Sonja Jozić

Faculty of Electrical Engineering, Mechanical Engineering and Naval Architecture, University of Split, Ruđera Boškovića 32, 21000 Split, Croatia; jkrolo@fesb.hr (J.K.); kgrgic00@fesb.hr (K.G.); sjozic@fesb.hr (S.J.)
* Correspondence: blela@fesb.hr

Abstract: The main aim of this research is to mathematically describe the influence of the processing parameters of metal foam production from machining chip waste. Using this method, metal foams were produced without a remelting step, which should be both economically and environmentally effective. Firstly, expensive metal powders were replaced with waste in the form of machining chips. Secondly, machining chip waste was recycled without any significant material losses, which usually occurs during conventional recycling (using the melting process). To describe the innovative process and to relate metal foam properties to foaming temperature, the blowing agent weight percentage, and foam density (controlled by foaming height), response surface methodology, and the design of experiments were used. The quality of the produced metal foams was evaluated by determination of density, yield strength, compression strength, plateau stress, energy absorption, pore perimeter, and pore inhomogeneity for specimens obtained following the experimental plan. It was proven that pore inhomogeneity increased in the range from 1.41 to 4.81 mm with a higher temperature and the addition of a foaming agent. However, higher energy absorption and yield strength were obtained with a higher temperature but a lower percentage of TiH_2. Despite the production from machining chips, pores were homogenous without significant cracks. These kinds of metal foams are comparable to commercial foams made of metal powders.

Keywords: aluminum foam; recycling; machining chips; response surface methodology

Citation: Krolo, J.; Lela, B.; Grgić, K.; Jozić, S. Production of Closed-Cell Foams Out of Aluminum Chip Waste: Mathematical Modeling and Optimization. *Metals* **2022**, *12*, 933. https://doi.org/10.3390/met12060933

Academic Editor: Man Seung Lee

Received: 3 May 2022
Accepted: 24 May 2022
Published: 28 May 2022

1. Introduction

Metal foams are lightweight cellular materials used due to their unique properties. There are many advantages of metal foam utilization, such as good overall energy, sound, and vibration absorption, as well as thermal and electrical properties [1]. A few important characteristics of metal foams are the high strength-to-weight ratio and large compressive strain at constant stress [2]. The usage of foams is also related to thermal insulation because of their low thermal conductivity [3]. Metal foams can be a desirable material for the transport industry due to the reduction in parts' weight and good energy absorption capability [4]. Because of their unique properties, they can be used in the aviation and defense sectors as well as in the naval and construction industries [5]. Metal foams can be made of various metals, such as aluminum, nickel, titanium, copper, magnesium, or steel [6]. They are usually divided into open- and closed-cell foams [7]. There are various commercial manufacturing procedures for their production. For closed-cell foams, two main production methods currently exist. One is based on the direct foaming of the liquid metal, and the other is based on powder metallurgy, i.e., on the foaming of solid precursors in the semisolid state [8]. In this research, a novel and cost-effective method for closed-cell aluminum foam production is presented. This novel process is based on the foaming of solid precursors made of aluminum machining chip waste. Usually, solid precursors are made by mixing a metal powder and blowing agent powder, followed by hot pressing or extrusion of the mixture. An optional cold pre-compaction step can be applied before hot pressing or extrusion. The final step is the foaming of the densified precursor by controlled heating to at least the melting point of the metal or alloy [9]. The advantage of the solid precursor route is that the precursor can expand in a heated mold, and foam with a complicated shape can be made [10]. The most common blowing agent for the foaming of closed-cell foams is TiH_2, which decomposes into Ti and H_2 and thus causes the formation of pores [3]. It is used because of the optimal balance between the temperature of its decomposition and the melting point of a metal alloy as well as its fast decomposition [11]. The other commonly used blowing agents are $CaCO_3$ and ZrH_2 [12]. There is also a mention of polymer methyl hydro siloxane used as a foaming agent [13]. Commonly used stabilizing agents, whose task is achieving a homogeneous pore structure, are SiC or Al_2O_3, as well as Ca and Mg. [14]. Banhart et al. investigated the production of aluminum foams that were made of aluminum alloy and TiH_2 with the powder metallurgy method. The influence of the percentage of the foaming agent was analyzed, and it was concluded that 1 (wt%) was the optimal value of the agent for good foaming characteristics [15]. Shiomu et al. presented a procedure of four sequential processes, specifically powder compaction, extrusion, foaming, and molding [16]. Cylindrical aluminum foam was produced by filling foam into a rapidly cooled steel pipe mold. The achieved distribution of relative density within the aluminum foam bar was in a range of 0.2–0.3. Papantoniou et al. researched the powder metallurgy route, where the influence of the powder morphology, the compaction pressure, and the foaming temperature were investigated. The highest foaming efficiency was observed when using fine aluminum powder for precursors produced with compaction pressures higher than 700 MPa and foaming temperatures of 750 °C and 800 °C [17].

In this research, aluminum foams were made directly from aluminum machining chips without remelting or their comminution into powder. Aluminum represents the second most consumed metal worldwide. It can be easily recycled, so it contributes to the reduction in pollution and provides electrical energy savings [18]. However, conventional recycling of aluminum alloy machining waste is problematic due to the high surface-to-mass ratio of the machining chips and their coverage with an oxide layer. Therefore, during the melting process in conventional recycling, there is a significant loss of material caused by the oxidation of the melted metal. Some loss is generated because of the inclusion of slags [19]. Additionally, losses can be produced during casting and processing, and the final material yield can be only around 60 (wt%) [20]. Furthermore, the aluminum foam production method presented in this paper can be considered both a novel recycling process and a novel metal foam production procedure. There is a similar alternative method for machining chip recycling without remelting, called solid-state recycling. With this method, reductions in the negative environmental impact and energy consumption are significant in comparison with conventional methods due to the high material and electricity savings [21]. Another important advantage of the method presented in this research is the replacement of expensive aluminum powder with low-cost aluminum machining chips, which directly influences the price of the produced metal foams. There were only a few studies that investigated the possibility of producing aluminum foams from chip waste. Hangai et al. used friction stir back extrusion to consolidate aluminum burrs and blowing agents into the solid precursor [22]. They foamed precursors inside steel tubes and produced cost-effective metal foams with homogeneous porosity. The compression properties of aluminum foams made out of burr-based precursors were similar to those of foams made from solid precursors [22]. Tsuda et al. investigated the possibility of producing aluminum foam from low-cost machined chip waste. They consolidated machining chips and blowing agents (TiH_2) by hot extrusion or compressive torsion. As claimed by the authors, oxides stabilize the cell structure in the conventional powder method, but when using machining chips, oxides are not so effective. Because of that, an Al_2O_3 stabilizer was added to the mixture [23]. According to the results of this research, better foaming characteristics and pore morphology were achieved when a solid-state precursor made by compression torsion was used instead of the extrusion process. The produced foams were comparable to those made from powder precursors [23]. Kanetake et al. showed that by using the same method as in the above-mentioned research, different kinds of aluminum alloy machined chips could be mixed to produce metal foams. It was concluded that an alloy that has lower solidus and liquidus temperatures would have earlier foaming. By combining aluminum alloys, an increase in porosity and a decrease in pore diameter can be achieved if the percentage of alloys that have a lower solidus temperature is higher [24].

Furthermore, there have only been a few attempts to create mathematical models that relate the manufacturing parameters of metal foams to their final properties and to mathematically optimize the production process. However, most of the research based on mathematical modeling was performed for the melting production route. Ali H. et al. produced metal foams by melting the metal matrix composite Duralcan F3S.20S and mixing it with the foaming agent (TiH_2) [3]. The authors researched the influence of the foaming temperature, percentage of the foaming agent, and mixing speed on average pore size and porous area using the Taguchi method. The ImageJ program was used to calculate the foams' microstructural output parameters. They concluded that the percentage of the foaming agent was the most influential parameter. With the increase in its content, there was an increase in pore size and a decrease in the porous area. A higher temperature and mixing speed led to a reduction in pore size and a decreased influence on the value of the porous area. The optimum settings of control factors, obtained to minimize the pore size and to increase the porosity characteristics, were 850 °C, 2000 rpm, and 1 (wt%) for the temperature, stirring speed, and weight percentage of the blowing agent, respectively [3]. Wang H. et al. used a two-step foaming method to produce aluminum alloy AlCu foams, where precursors were made using the melting route and the addition of TiH_2 powder and Ca particles (this was considered the first foaming step). Partially foamed specimens were treated as the precursor for the subsequent second foaming step. Using the Taguchi method, they showed that processing parameters, including the holding time, foaming temperature, and their mutual interaction during the second foaming, could affect the final cellular structure features, such as the porosity content, average diameter, pore distribution uniformity, and sphericity. Quantitative analysis indicated that a holding time below 5 min and foaming temperature above 760 °C during the second foaming step could fabricate AlCu alloy foams with the proper cellular structure and energy absorption capability [25]. Rajak D.K. et al. researched closed-cell foam made of AlSi17 aluminum alloy, which was also fabricated through the melting production route using calcium powder as a thickening agent and TiH_2 as a foaming agent, along with the addition of 10 (wt%) SiC particles. They researched the potential of a neural network approach to correlate and predict the influence of the compression strain rate, average pore size, and relative density on plateau stress [14]. The artificial neural network approach was also used in other research where the melting route was used to obtain metal foams [26].

As stated in the above-mentioned research, the mathematical modeling approach has great benefits in the description of the influence of manufacturing parameters on metal foam properties, especially in non-commercialized and novel foam production procedures. However, according to the literature available to the authors, there is no description of the production of chip-based foam using a mathematical modeling approach. Therefore, in this research, response surface methodology was utilized to describe the influence of the foaming temperature, foam density change (regulated by height change), and weight percentage of titanium hydride as the blowing agent on the chip-based metal foam quality. To evaluate the quality of the produced metal foams, the output parameters were foam density, energy absorption, yield strength, plateau stress, pore perimeter, and pore inhomogeneity.

Finally, this research presents the mathematical modeling of the production of closed-cell metal foams aimed at recycling aluminum chips, and this approach was not presented in the literature before.

2. Materials and Methods

2.1. Design of Experiments

In this research, design of experiments and response surface methodology approaches were selected to determine the influence of the metal foam production parameters and their mutual interaction on metal foam mechanical and physical properties and their pore morphology. Due to the metal foam's complex behavior during foaming and to reduce the number of experiments, the Box Behnken experimental design was selected. Regression analysis and variance analysis were used to derive mathematical models that can describe the above-mentioned influence. The weight percentage of the blowing agent (TiH_2), foaming temperature range, and specimen height change were selected as influencing parameters. To determine which temperature range and amount of foaming agent are needed to successfully produce foams from chip-based precursors, it was necessary to conduct preliminary experiments. In the introduction, it was already mentioned that there is a great research gap in metal foam production from machining chips, and therefore, the appropriate processing parameters are quite unknown. In Table 1, selected temperature ranges and TiH_2 weight percentages for foam growth testing and density evaluation are shown. Metal foam growth was measured using the OMRON ZX1-LD300A61 5M optical displacement sensor (Omron Corporation, Kyoto, Japan) in the open metal foam mold (Figure 1a). The selected alloy was A380 (EN AC AlSi9Cu3(Fe)) obtained from Aluminij Industries d.o.o., Bosnia and Hercegovina. The chemical composition of the alloy was: 9.1% Si; 1.3% Fe; 3.2% Cu; 0.5% Mn; 0.1% Mg; 0.41% Ni; 2.1% Zn; 0.25% Sn; 0.5% other metals. A more detailed explanation of the precursor production procedure is provided in the Experimental Procedure section. Foam growth versus time is visible in Figure 1b. According to the results presented in Table 1 and Figure 1b, it is visible that for the selected temperatures (590 °C and 610 °C), 0.5 (wt%) of TiH_2 is an appropriate selection to achieve good foaming in a reasonable time range (specimens 3 and 4). Specimen 2, which was foamed from the precursor with 0.25 (wt%) TiH_2, was successfully foamed at 610 °C, but at 590 °C, the foaming process was quite long (Figure 1b, specimen 1), and it is not possible to achieve a density below 0.909 g/cm^3 in that time range (Table 1).

Table 1. Preliminary foaming parameters for metal foam growth evaluation.

Specimen	Blowing Agent TiH_2 (wt%)	Temperature (°C)	Density (g/cm^3)	Relative Density
1	0.25	590	0.909	0.34
2	0.25	610	0.804	0.3
3	0.5	590	0.688	0.26
4	0.5	610	0.764	0.28

Therefore, in the experimental plan, the selected (wt%) of the TiH_2 blowing agent was from 0.5 (wt%) to 1.5 (wt%), while the temperature range was from 590 °C to 610 °C. Finally, the third parameter was foam height, which was in the range from 40 mm to 70 mm. The foam height change in the foaming mold should have a direct impact on foam volume and density changes, among other properties. The authors of this paper decided to evaluate the possibility of regulating density with the change in the metal foam height during foaming. Different metal precursor foaming heights do not necessarily mean that homogeneous metal foams with different densities will be obtained. There is a possibility of producing foams in which the lower and upper parts have quite different densities. In this study, all metal foams were cut in the same manner, so if the density homogeneity problem occurred, the mathematical model would not be significant. Therefore, as an input parameter, metal foam height was selected instead of metal foam density. According to the Box Behnken design, in total, 17 experimental points were created using "Design Expert" computer software (version 10, Stat-Ease Inc., Minneapolis, MN, USA). These are visible in Table 2, and experimentally determined output parameters (density, energy absorption, plateau stress, yield strength ($Rp_{0.2}$), pore perimeter, and pore inhomogeneity) are also shown.

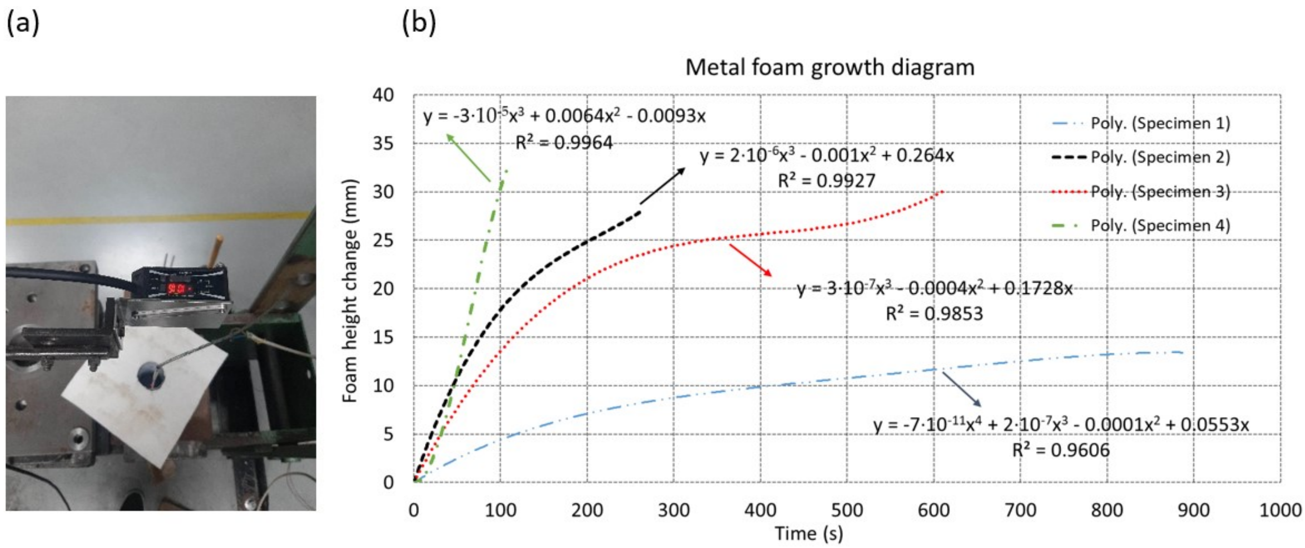

Figure 1. (**a**) Metal foam growth measurement. (**b**) Metal foam growth versus time for different foaming parameters.

Table 2. Design of experiments and properties of chip-based aluminum foams.

Level of Exp. Run	Blowing Agent TiH_2 (wt%)	Foam Height (mm)	Temperature (°C)	Density (g/cm^3)	Energy Absorption (MJ/m^3)	Plateau Stress (MPa)	$Rp_{0.2}$ (MPa)	Pore Perimeter (mm)	Pore Inhomogeneity (S.D.)
1	1.00	55.00	600.00	0.813	16.758	34.6	32.0	4.8	1.61
2	0.50	40.00	600.00	1.021	21.7823	23.5	58.0	4.3	2.05
3	1.00	55.00	600.00	0.764	14.6647	30.0	32.7	5.2	2.14
4	0.50	70.00	600.00	0.651	11.8967	25.0	25.2	6.2	2.61
5	1.00	40.00	590.00	1.148	31.3413	62.3	64.3	3.2	1.41
6	1.00	55.00	600.00	0.821	17.3468	35.7	35.7	5.4	2.91
7	1.00	40.00	610.00	0.993	22.3228	44.4	50.9	4.3	2.54
8	1.00	70.00	590.00	0.640	11.2354	23.5	25.4	5.5	1.90
9	1.50	40.00	600.00	0.930	19.8079	39.5	38.0	4.8	1.72
10	0.50	55.00	590.00	0.786	15.4102	29.5	38.7	5.4	3.33
11	1.50	55.00	590.00	0.753	14.8613	29.1	41.4	5.2	2.19
12	1.00	70.00	610.00	0.703	12.5716	25.4	25.3	4.8	2.20
13	1.50	55.00	610.00	0.749	17.5522	35.8	33.0	4.8	4.81
14	1.00	55.00	600.00	0.811	15.6664	32.6	23.7	5.1	2.59
15	1.00	55.00	600.00	0.777	15.6003	32.1	30.1	6.1	2.87
16	0.50	55.00	610.00	0.853	11.269	24.8	14.4	7.4	2.11
17	1.50	70.00	600.00	0.610	10.8603	21,8	25.9	5.2	2.10

Detailed information on calculations of energy absorption, plateau stress, and yield strength $Rp_{0.2}$ can be found in Reference [27].

2.2. Experimental Procedure

The main aim of this research was to determine the recycling possibility of A380 (EN AC AlSi9Cu3(Fe)) aluminum alloy machining chips with the purpose of creating cost-effective and quality metal foams. Aluminum alloy A380 was selected for this research due to its wide use in the automotive industry and high-pressure die casting technology [28]. The selected alloy has good casting characteristics, and it is mainly used to produce complex castings with thin walls that are exposed to dynamic loads and for mold castings for machine and engine parts, cylinder heads, parts of electric motors, and bearing blocks. Because of the versatile use of the A380 alloy, there is a lot of generated machining chip waste. Furthermore, in metal foam production, the usage of casting alloys instead of wrought alloys can reduce the foaming temperature by reason of the lower solidus line, which should result in a more energy-efficient process. To determine solidus and liquidus lines for the selected alloy, DTA analysis was performed on a TG/DTG-DTA Pyris Diamond measurement device (PerkinElmer, Inc., Waltham, MA, USA). Solidus and liquidus temperatures were determined to be 497 °C and 600 °C, respectively.

In this research, machining chips were obtained on the Spinner VC 560 vertical machining center (SPINNER GmbH, München, Germany). To avoid contamination with cooling and lubrication fluid, a dry face milling process was performed using a tool composed of the WALTER tool holder (Walter AG, Tübingen, Germany) with designation M4132-032-W32-02-09 and the SDHT09T304-G88 WK10 cutting insert. Machining parameters were selected as follows: a_p = 1.5 mm, v_c = 120 m/min, and f = 0.1 mm/tooth.

The first step to prepare the precursor was chip mixing with a blowing agent. For the blowing agent, TiH_2 in the form of 44-micron powder was selected, as it is the most used agent in aluminum foam production [8]. According to the DTA curves obtained in this research with the same measurement device as mentioned above, the expected temperature for the decomposition of TiH_2 and hydrogen gas release ranges from 350 °C to 740 °C. However, the most intense TiH_2 decomposition starts at 550 °C and finishes at 630 °C. To obtain a homogeneous distribution of the blowing agent (TiH_2) over machining chips during mixing, finely dispersed distilled water droplets were introduced into the mixture. Machining chips were weighed to the same mass of 150 g after mixing with the appropriate TiH_2 (wt%). According to the experimental plan (Table 2), they were compacted with 0,3 MN force in a cylindrical steel tool with an inner channel diameter of 38 mm and a height of 150 mm. The compacted sample was 38 mm in diameter and 68 mm in height (Figure 2a). Compaction was performed on a hydraulic press, while the force was measured with the HBM load cell C6A 1MN sensor (HBM, Darmstadt, Germany). Chip-based billets, formed with the appropriate amount of the blowing agent, were preheated for 20 min at 400 °C and directly hot extruded at 400 °C with a 7.1 extrusion ratio. An extrusion temperature of 400 °C was selected to prevent total TiH_2 decomposition and to preserve the blowing gas pressure during precursor foaming at higher temperatures. A flat die with an orifice diameter of 15 mm was used in the extrusion process. The punch speed was 1 mm/s. The temperature was controlled using the Omron E5CC temperature regulator (Omron Corporation, Kyoto, Japan) and G3PE-225B DC12-24 relay (Omron Corporation, Kyoto, Japan). Extrusion pressure was measured with an HBM P15RVA1/500B pressure gauge transducer (HBM, Darmstadt, Germany). Obtained precursors in the form of round bars were about 300 mm long, and they were cut on smaller 35 mm length precursors, which can be seen in Figure 2b.

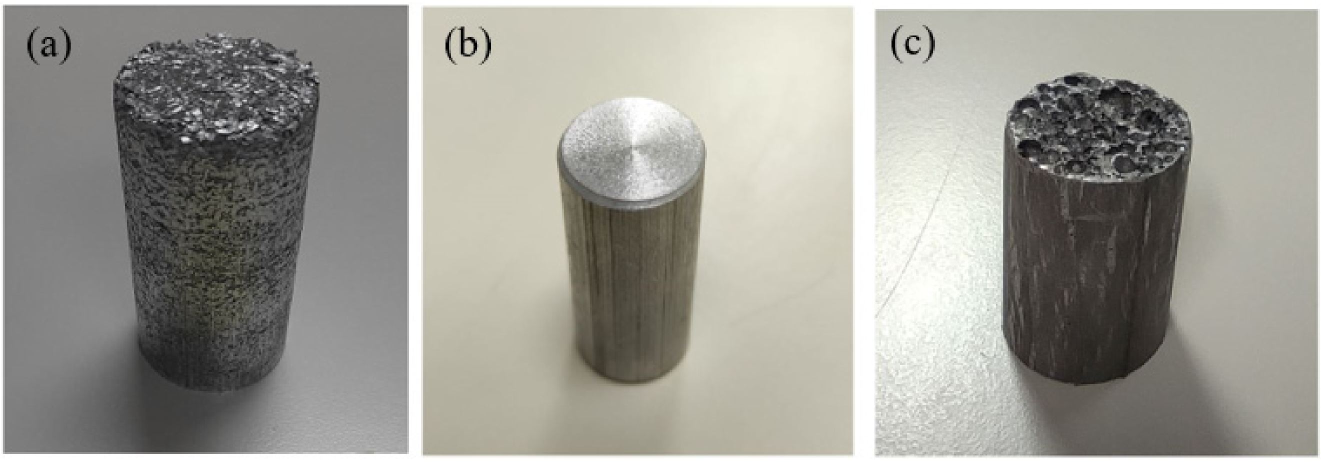

Figure 2. Material flow during chip-based foam production: (**a**) billet, (**b**) precursor, and (**c**) metal foam.

Finally, to produce metal foams from aluminum machining chip-based precursors, a mold made of 42CrMo4 steel with 22 mm diameter and 100 mm height was prepared. Before heating the mold, the inner surface was covered with boron nitride to prevent aluminum from sticking to it. The steel mold was heated with an OMEGALUX CRFC

46/240-A ceramic heater (Omega Engineering Inc., Norwalk, CT, USA) at the appropriate temperature according to the experimental plan for each sample (Table 2). The temperature was measured with the Omron E5CC temperature regulator and the type K thermocouple probe (Omega Engineering Inc., Norwalk, CT, USA). To control the foam height change, which is directly related to volume and density changes, the OMRON ZX1-LD300A61 5M optical displacement sensor (Omron Corporation, Kyoto, Japan) was used. When the desired foam height was reached, the steel mold was cooled with sprayed water. Because the precursors were heated at temperatures that correlate to the semisolid temperatures of the precursor base material, foam growth was stopped at the desired height in a fairly short time. After obtaining 17 aluminum foam samples, they were all cut at the same height of 33 mm to achieve a height-to-diameter ratio of 1.5, which is needed for compression testing (Figure 2c).

The next step was density measurement, as well as the pore size and morphology evaluation of each sample. For the density measurement, a Steinberg Systems SBS-TW-500/10 laboratory balance (Steinberg Systems, Warsaw, Poland) was used, while volume was calculated from each specimen's dimensions.

3. Results and Discussion

3.1. Pore Size and Inhomogeneity Analysis

Pore size is expressed as pore perimeter measurements on two cut surfaces using the Profilm3D 3D optical profilometer (KLA Corporation, Milpitas, CA, USA) and ImageJ image analysis software (version 1.53r, License: Public Domain, BSD-2). The pore inhomogeneity index is simply expressed as the standard deviation of the pore perimeter measurement. For each sample, at least 35 pores were measured. However, the number of measured pores depended on the pore size and specimen density. Three-dimensional optical profilometry was also used to evaluate the obtained metal foam quality. In Figure 3, line profile measurements can be seen for cross-sections at 4 mm, 8 mm, 12 mm, and 16 mm from the metal foam bottom edge. On the profile lines, some points are highlighted with X and Y coordinates so that cell wall thickness and pore depth can easily be calculated. According to the 3D scanning results, foam cell walls were quite homogeneous without any significant cracks. Cells were homogeneously dispersed across the metal foam cross-section, and cell wall thickness was uniform for all created pores. Three-dimensional optical profilometry can provide a unique insight into the created cell wall size and geometry with precise measurement ability.

3.2. Compression Test

Figure 4a shows 8 compression test curves randomly selected out of 17 curves obtained after the experimental plan (Table 1) was carried out. According to Figure 4a, the engineering stress versus strain curves have a characteristic shape that consists of three characteristic areas: the first stage, which is elastic deformation; the second stage, where plateau stress appears; and the third stage, where densification of the metal foam occurs [1]. The characteristic shape of the compression test diagrams is the first indication that homogeneous chip-based metal foams were successfully produced. According to the results, the plateau stress, energy absorption, and yield strength for all 17 samples were in ranges from 21.8 MPa to 62.3 MPa, 10.9 MJ/m^3 to 31.3 MJ/$m^{3,}$ and 14.4 MPa to 64.3 MPa, respectively (Table 2).

In the following sections of the paper, derived mathematical models and response surfaces for foam density, energy absorption, yield strength, pore perimeter, and pore inhomogeneity are described. The foam plateau stress could not be described with the statistically significant mathematical model, so it was suggested to use the mean value, which is 32.3 MPa with a 9.6 MPa standard deviation (Figure 4b).

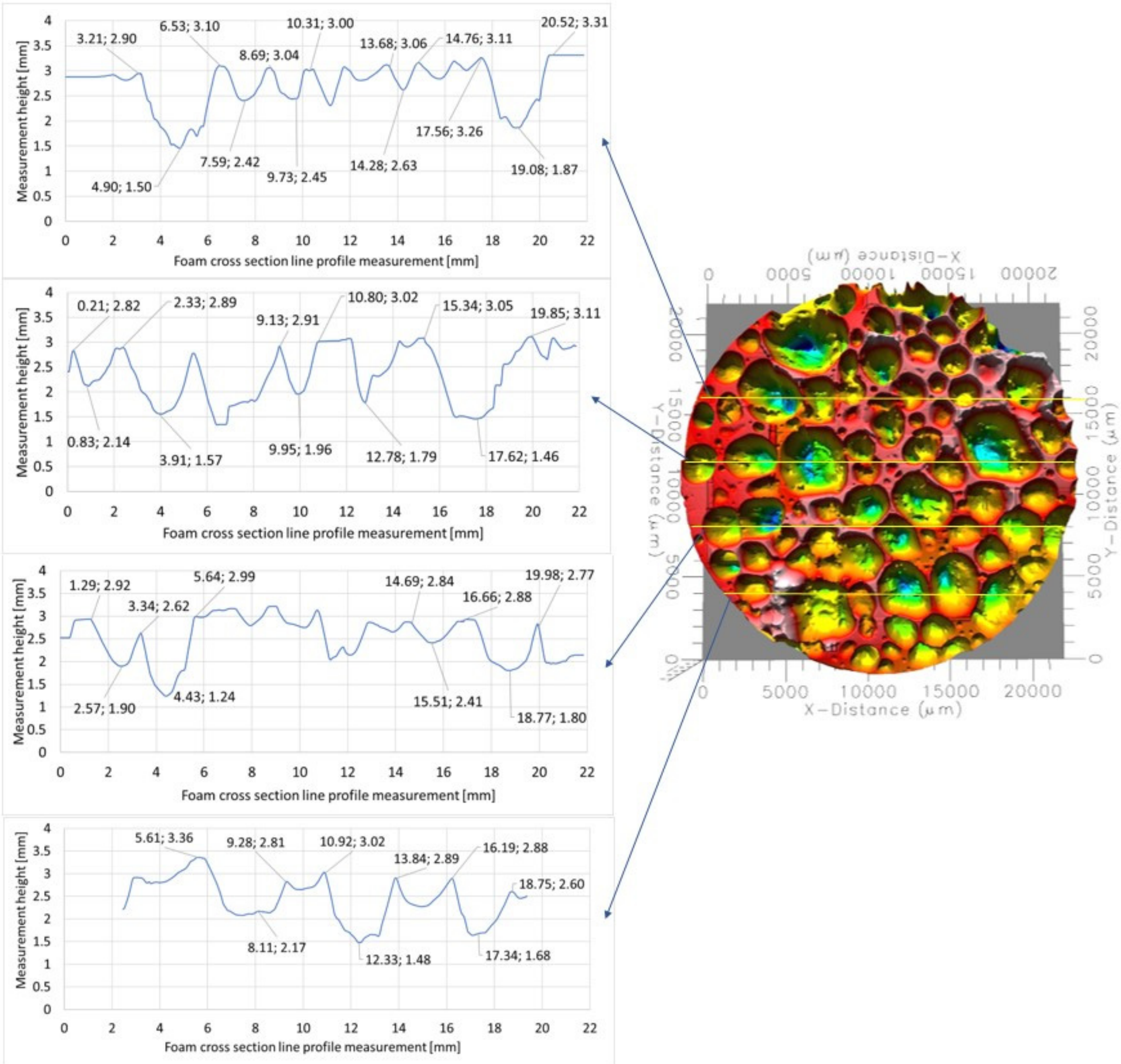

Figure 3. Three-dimensional surface of metal foam with a density of 0.65 g/cm^3 and selected cross-section profile line measurements.

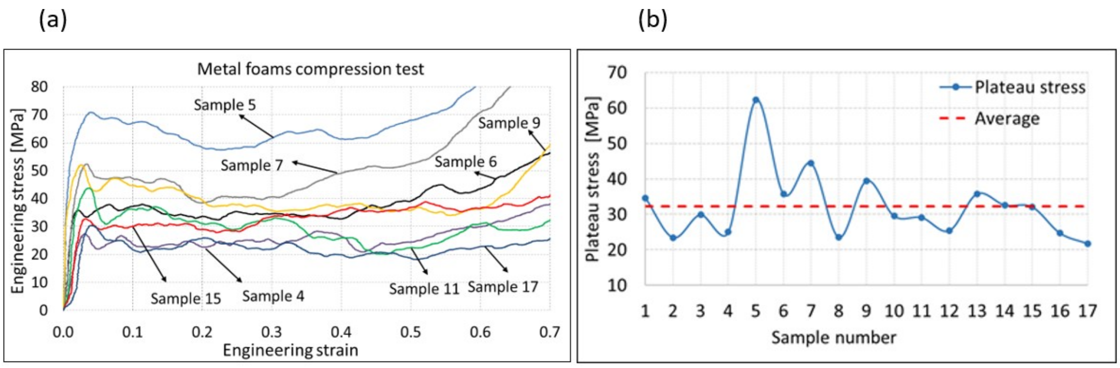

Figure 4. (**a**) Compression test diagram of eight samples randomly selected from the design of experiments. (**b**) Plateau stress values for all samples.

3.3. Regression Analysis for Density

According to the regression analysis (RA) and variance analysis (ANOVA), a quadratic mathematical model that presents the impact of the blowing agent (wt%), temperature range, and foam height (volume change) on the chip-based foam density was formulated. For better understanding, from now on, *A*, *B*, and *C* denote blowing agent (wt%), foam height [mm], and temperature [°C], respectively. ANOVA indicated that, in this case, *A*, *B*, *BC*, A^2, and B^2 were significant model terms. Model quality can be evaluated based on *R-Squared*, *Adj R-Squared*, *Pred R-Squared*, and *Adeq Precision* values. The quadratic mathematical model obtained with RA had a strong coefficient of determination *R-Squared* = 0.96. The high *R-Squared* value indicates that the predicted density values, based on the model, are in very good agreement with the actual experimental values. Furthermore, *Adj R-Squared* and *Pred R-Squared* were 0.94 and 0.84, respectively. Good agreement between *Adj R-Squared* and *Pred R-Squared* is important because it prevents the overfitting of the model. Finally, *Adeq Precision* for this model was 22.5. *Adeq Precision* measures the signal-to-noise ratio, and a ratio greater than 4 is desirable. The quadratic mathematical model in terms of actual factors was adopted as follows:

$$\begin{aligned} \mathit{Density}\ [\mathrm{g/cm^3}] &= 14.18130 + 0.24208 \cdot A - 0.25227 \cdot B - 0.020234 \cdot C \\ &+ 3.61167 \cdot 10^{-4} \cdot B \cdot C - 0.15466 \cdot A^2 + 2.10596 \cdot 10^{-4} \cdot B^2 \end{aligned} \tag{1}$$

Figure 5a–d show the graphical presentation of Equation (1) for a constant foaming temperature of 590 °C, 1 (wt%) of the blowing agent, and foaming heights of 40 mm and 70 mm, respectively.

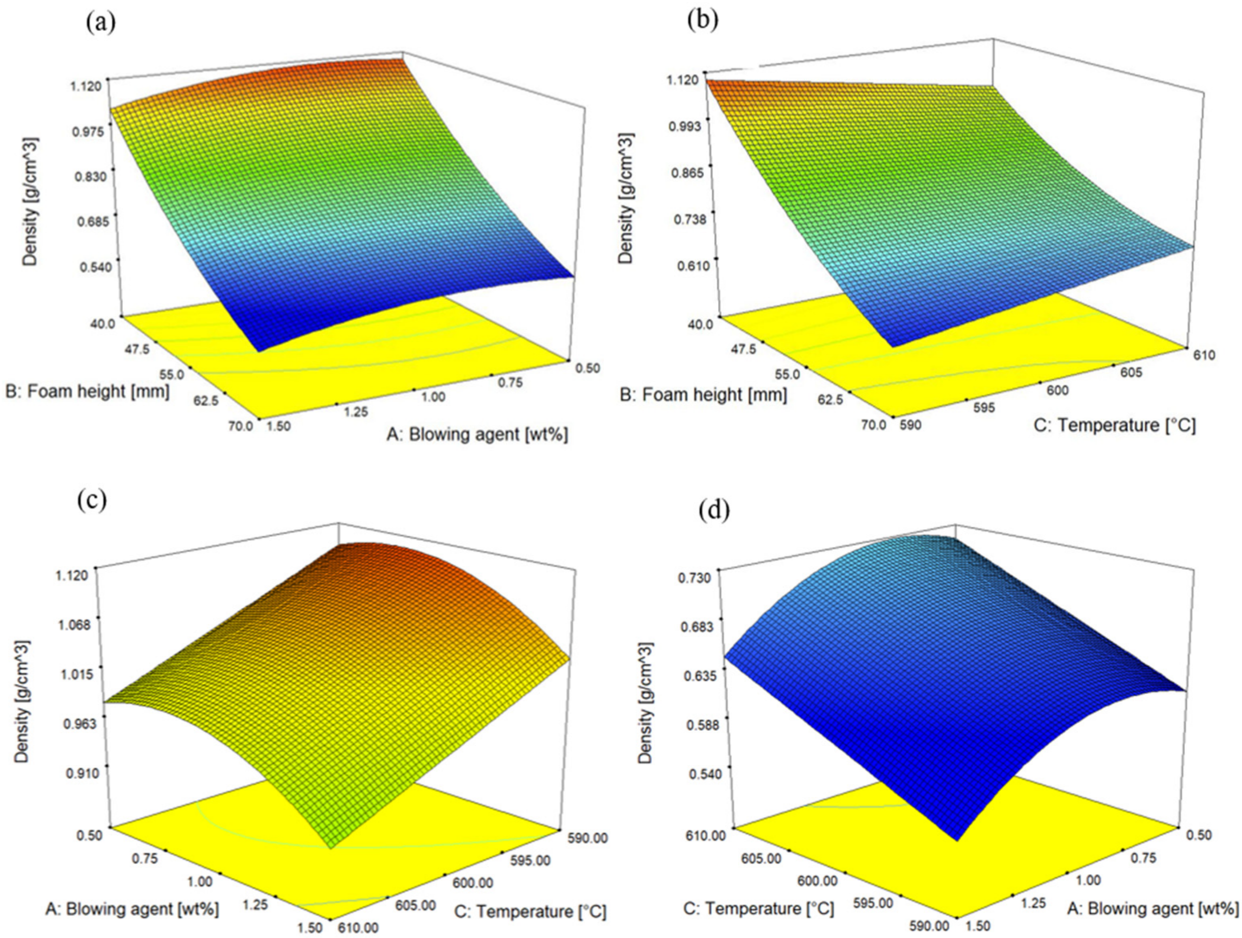

Figure 5. (**a**) Influence of foam height and blowing agent (wt%) on foam density for constant foaming temperature of 590 °C. (**b**) Influence of foam height and foaming temperature on density for 1 (wt%) TiH_2. (**c**,**d**) Influence of the foaming temperature and blowing agent (wt%) for constant foam heights of 40 mm and 70 mm, respectively.

The surface in Figure 5a shows how the foam density changes with different foam heights. In particular, the surface in Figure 5b indicates that for 1 (wt%) of the agent and a foam height of 40 mm, a higher foaming temperature will result in lower foam density, while for a 70 mm foam height, a lower foaming temperature will result in lower foam density. Figure 5c,d indicate a similar influence of the temperature for all weight percentages of the blowing agent. Furthermore, according to Figure 5c,d, increasing the amount of the blowing agent by more than 1 (wt%) will slightly reduce the foam density for a constant foam height and the whole temperature range.

3.4. Regression Analysis for Energy Absorption and Yield Strength

In accordance with the regression analysis (RA) and variance analysis (ANOVA), a quadratic mathematical model for the relation of the processing parameters to the energy absorption of the chip-based foams was developed. ANOVA indicated that, in this case, B, BC, and A^2 were significant model terms. The quadratic mathematical model obtained with RA had a coefficient of determination *R-Squared* = 0.93. Furthermore, *Adj R-Squared* and *Pred R-Squared* were 0.87 and 0.56, respectively. Finally, *Adeq Precision* for this model was 14.3. The quadratic mathematical model in terms of actual factors was adopted as follows:

$$\begin{aligned}\textit{Energy absorption}\ [\mathrm{MJ/m^3}] = 101.26993 - 25.00468 \cdot A - 1.22538 \cdot B - 0.15442 \cdot C \\ + 0.045157 \cdot A \cdot C + 1.77889{\cdot}10^{-3} \cdot B \cdot C - 0.99577 \cdot A^2 + 9.97500{\cdot}10^{-4} \cdot B^2\end{aligned} \tag{2}$$

Figure 6a–d show the graphical presentation of Equation (2) for a constant foaming temperature of 590 °C, 1 (wt%) of the blowing agent, and foaming heights of 40 mm and 70 mm, respectively. According to Figure 6a and ANOVA, the most influential factor on foam energy absorption was foam height. This was expected due to the connection between foam height and density. However, in accordance with Figure 6b,c and ANOVA analysis, for samples foamed at a 40 mm height with 1 and 0.5 (wt%) of TiH_2, a 590 °C foaming temperature is much more desirable than 610 °C for the production of foams with higher energy absorption capability. There was a significant drop in energy absorption capability when 610 °C and 0.5 (wt%) of TiH_2 were used. Overall, the highest energy absorption was achieved when 590 °C and 0.5 (wt%) of TiH_2 were used for metal foams with a 40 mm height. According to Figure 6d, quite different behavior was observed for samples foamed at a 70 mm height. In this case, when using 0.5 (wt%) of TiH_2, the temperature change did not influence energy absorption capability. However, when 1 or 1.5 (wt%) of TiH_2 was used, an increase in energy absorption was observed when a 610 °C temperature was used instead of 590 °C.

Furthermore, on the basis of the regression analysis (RA) and variance analysis (ANOVA), a linear mathematical model for the relation of the processing parameters to the yield strength of the chip-based foams was developed. ANOVA indicated that, in this case, *B* was a significant model term, which means that the specimens' foaming height had the most influence on the foams' yield strength. According to Figure 5 and Equation (1), the obtained foam density is strongly dependent on foaming height; therefore, yield strength increases with decreasing foaming height. Furthermore, *R-Squared*, *Adj R-Squared*, and *Pred R-Squared* for the obtained model were 0.66, 0.58, and 0.35, respectively. Finally, *Adeq Precision* for this model was 9.3. To keep this paper simple and concise, only the derived linear mathematical model in terms of actual factors is presented as follows:

$$\textit{Yield strength}\ [\mathrm{MPa}] = 430.97483 + 0.51821 \cdot A - 0.91189 \cdot B - 0.57728 \cdot C \tag{3}$$

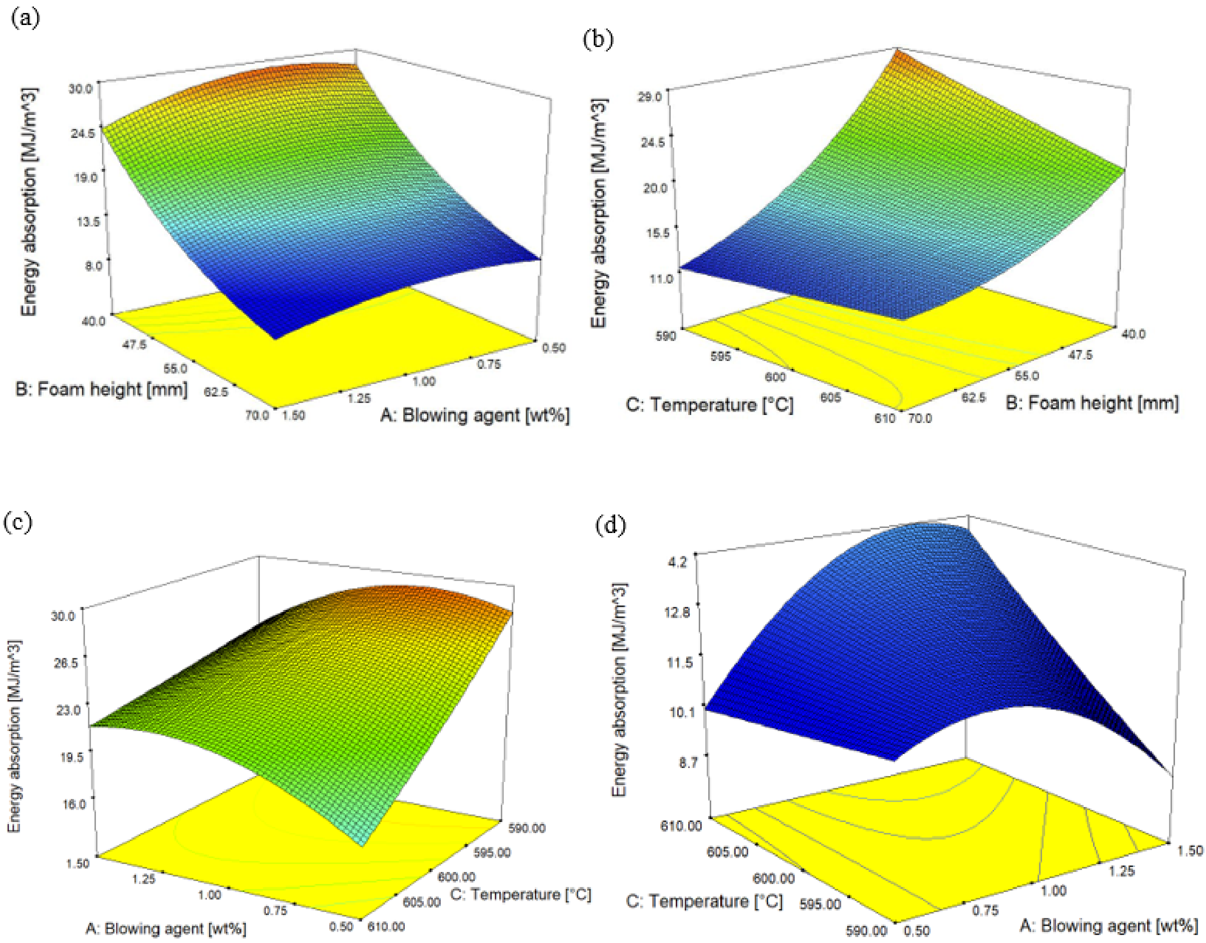

Figure 6. (**a**) Influence of foam height and blowing agent (wt%) on energy absorption for constant foaming temperature of 590 °C. (**b**) Influence of foam height and temperature on energy absorption for 1 (wt%) TiH_2. (**c**,**d**) Influence of the foaming temperature and blowing agent (wt%) for constant foam heights of 40 mm and 70 mm, respectively.

3.5. Regression Analysis for Pore Size

Figure 7 shows the different pore morphologies for eight samples randomly selected from the experimental plan. In Figure 7, it is visible that for selected samples and different metal foam production parameters (Table 2), significantly different pore sizes and distributions appear. However, the pore distribution in all samples seems homogeneous, without any significant base material domains or large pores. The statistical analysis presented in the next section shows that pore size and homogeneity depend on the production parameters.

According to the regression analysis (RA) and variance analysis (ANOVA), a quadratic mathematical model for the relation of the processing parameters to the pore size of the chip-based foams was developed. ANOVA indicated that, in this case, A, B, AC, and B^2 were significant model terms. The quadratic mathematical model obtained with RA had a coefficient of determination *R-Squared* = 0.81. Furthermore, *Adj R-Squared* and *Pred R-Squared* were 0.66 and 0.22, respectively. Finally, *Adeq Precision* for this model was 10.7. The quadratic mathematical model in terms of actual factors was adopted as follows:

$$\begin{aligned} \textit{Pore perimeter}\ [\text{mm}] = {} & -184.62526 + 67.67789 \cdot A + 2.07405 \cdot B + 0.30120 \cdot C \\ & - 0.12130 \cdot A \cdot C - 2.79167{\cdot}10^{-3}{\cdot}\ B \cdot C + 2.12205 \cdot A^2 - 3.24550{\cdot}10^{-3}{\cdot}\ B^2 \end{aligned} \quad (4)$$

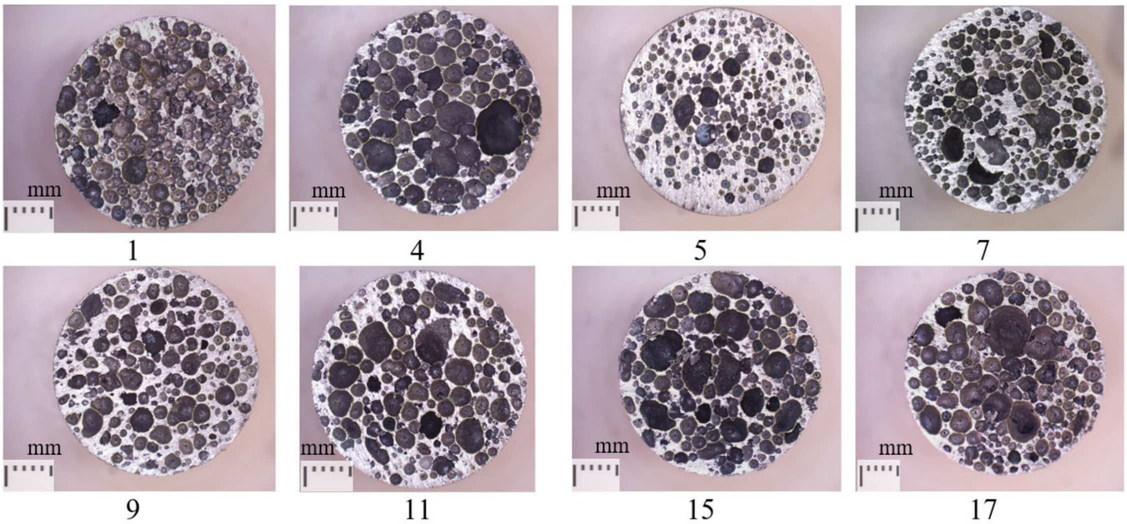

Figure 7. Different pore morphologies for eight samples randomly selected from the experimental plan (the numbers below photos denote experimental points).

Figure 8a–d show the graphical presentation of Equation (4) for a constant foaming height of 55 mm, a temperature of 610 °C, and blowing agent (wt%) of 0.5 and 1.5, respectively.

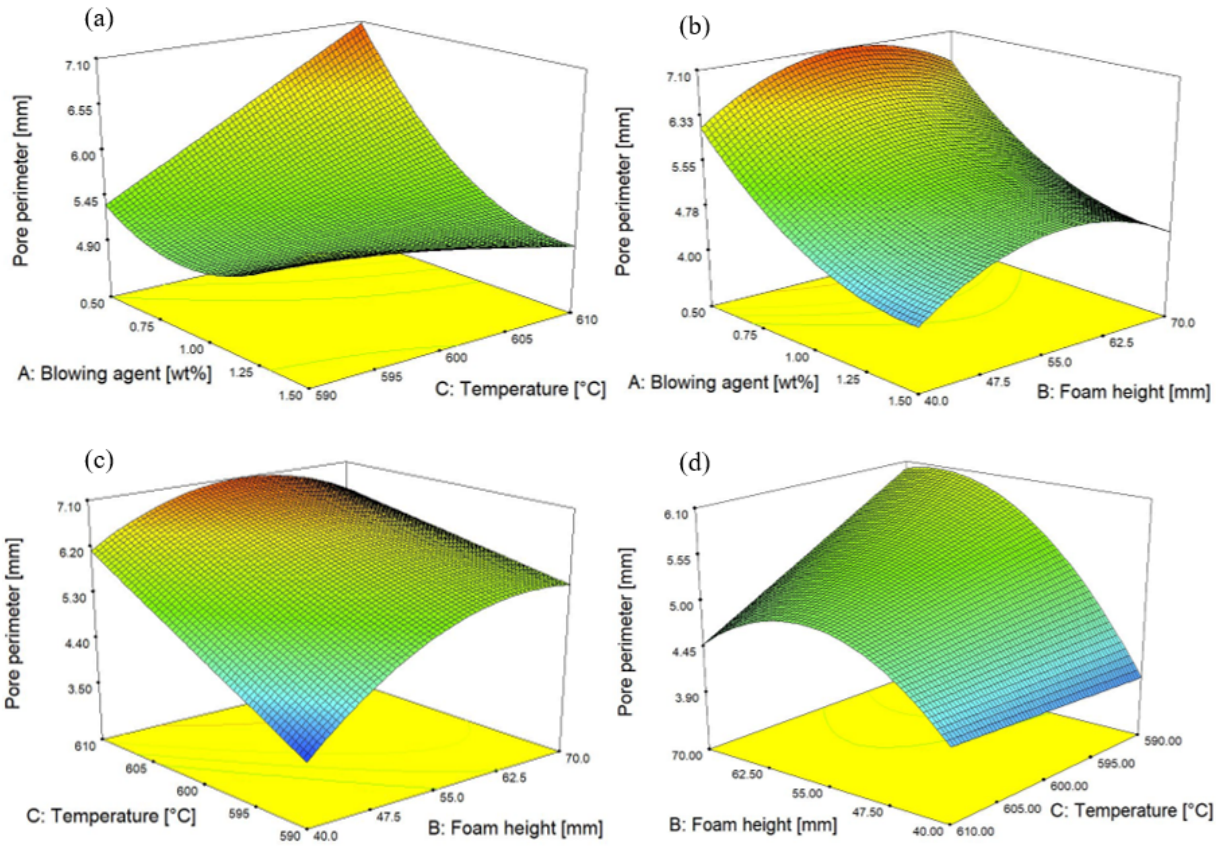

Figure 8. (**a**) Influence of blowing agent (wt%) and temperature on foam pore perimeter for a constant foaming height of 55 mm. (**b**) Influence of blowing agent (wt%) and foam height on foam pore perimeter for a constant foaming temperature of 610 °C. (**c**,**d**) Influence of the foaming temperature and foam height for constant (wt%) blowing agent of 0.5 and 1.5, respectively.

According to ANOVA and Figure 8a,b, it seems that the foam pore perimeter increases with a lower amount of the blowing agent. The foam pore perimeter was highest with 0.5 (wt%) of the blowing agent and a 610 °C foaming temperature (Figure 8a). It seems that at a 610 °C temperature, the perimeter of the foam pores increases with the decrease in the blowing agent amount for all foaming heights (Figure 8b). This was not the case for 590 °C and 600 °C, probably due to the increase in the semisolid slurry viscosity and the higher amount of the solid phase. According to the diagram presented in Figure 1, the foaming process duration is highly dependent on both the foaming temperature and the amount of the blowing agent. For samples with 0.5 (wt%) of foaming agent, the longest foaming duration for the whole temperature and foaming height ranges was observed. Furthermore, Figure 8c confirms the above-mentioned conclusion and shows that for 590°C and 600 °C temperatures and 0.5 (wt%) of the blowing agent, an increase in foam height results in a pore perimeter increase. Figure 8d shows that for 1.5 (wt%) of the blowing agent, the foaming temperature does not influence the pore perimeter when 40 mm foaming height was achieved, while for a foaming height of 70 mm and foaming temperature of 590 °C, a larger pore perimeter was achieved because of the prolonged heating time and therefore the merging and growth of pores.

3.6. Regression Analysis for Pore Inhomogeneity

According to the regression analysis (RA) and variance analysis (ANOVA), a quadratic mathematical model for the relation of the processing parameters to the pore inhomogeneity of the chip-based foams was formulated. ANOVA indicated that, in this case, AC and B^2 were significant model terms. The quadratic mathematical model obtained with RA had a coefficient of determination *R-Squared* = 0.74. Furthermore, *Adj R-Squared* and *Pred R-Squared* were 0.60 and 0.12, respectively. Finally, *Adeq Precision* for this model was 9.3. The quadratic mathematical model in terms of actual factors was adopted as follows:

$$\begin{aligned} &\text{P}\textit{ores inhomogeneity}\ (S.D.) = +87.96487 - 118.03328 \cdot A + 0.34451 \cdot B - 0.15614 \cdot C \\ &+ 0.19155 \cdot A \cdot C + 1.64126 \cdot A^2 - 3.04860 \cdot 10^{-3} \cdot B^2 \end{aligned} \tag{5}$$

Figure 9a–d show the graphical presentation of Equation (5) for a constant foaming height of 55 mm, a temperature of 610 °C, and blowing agent (wt%) of 0.5 and 1.5, respectively.

According to Figure 9a, pore inhomogeneity increases with a higher amount of the blowing agent and the highest foaming temperatures. This was probably due to the lower semisolid slurry viscosity and higher amount of the blowing agent, which caused some pores to coagulate or to grow rapidly because of the increased blowing gas pressure. This indicates that pore homogeneity will be reduced if both 1.5 (wt%) of the blowing agent and 610 °C foaming temperature are selected. Figure 9b shows that, for all foaming heights (foam densities) and 610 °C foaming temperature, foam pore inhomogeneity will be reduced if 0.5 (wt%) of the blowing agent is used. According to Figure 9c, for 0.5 (wt%) of the blowing agent and the whole range of foaming height, pore inhomogeneity decreases with the increase in foaming temperature from 590 °C to 610 °C. On the other hand, for 1.5 (wt%) of the blowing agent, pore inhomogeneity decreases significantly as foaming temperature decreases from 610 °C to 590 °C (Figure 9d).

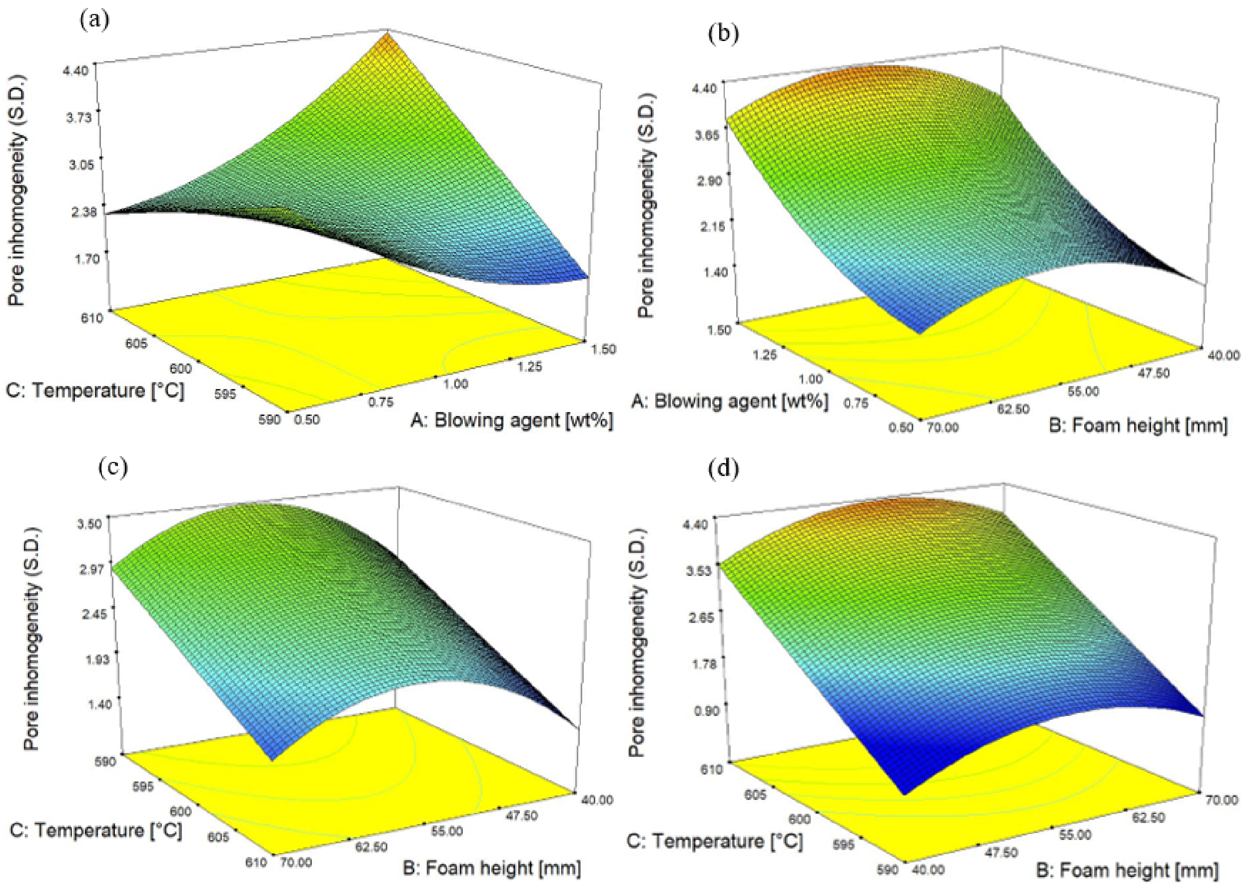

Figure 9. (**a**) Influence of foam height and temperature on foam pore inhomogeneity for a constant foaming height at 55 mm. (**b**) Influence of blowing agent (wt%) and foam height on foam pores inhomogeneity for the constant foaming temperature of 610 °C. (**c**,**d**) Influence of the foaming temperature and foam height for constant (wt%) of blowing agent of 0.5 and 1.5, respectively.

3.7. Optimization of Foam Properties

It is shown that the presented mathematical modeling and statistical analysis approaches can be successfully used to describe the metal foam production procedure and the complex influence of process parameters on metal foam properties. Based on the derived models' process parameters, optimization can be performed. In this research, due to the large range of the input and output parameters, the graphical optimization method was used. Limit values were selected for density, energy absorption, and pore inhomogeneity. The upper density limit was 0.65 g/cm^3, the lower energy absorption limit was set to 10 MJ/m^3, and the pore inhomogeneity's upper limit was set to be 2 mm, while the pore perimeter and yield strength had no limits for this example. Figure 10 shows the possible parameter ranges to obtain metal foam with such characteristics for a foaming temperature of 590 °C. For the selected point in Figure 10, the metal foam should have density, energy absorption, yield strength, pore perimeter, and pore inhomogeneity values of 0.63 g/cm^3, 11.82 MJ/m^3, 27.9 MPa, 5.3 mm, and 1.84, respectively. This should be achieved if metal foam with 0.94 (wt%) of the blowing agent is foamed at 590 °C until reaching a 69 mm height. These limits were selected to create metal foam with low density but with good homogeneity and energy absorption capability, which could be used, for example, as a crash absorber in the automotive industry. Another optimization can also be easily performed depending on the application for which the metal foam will be used.

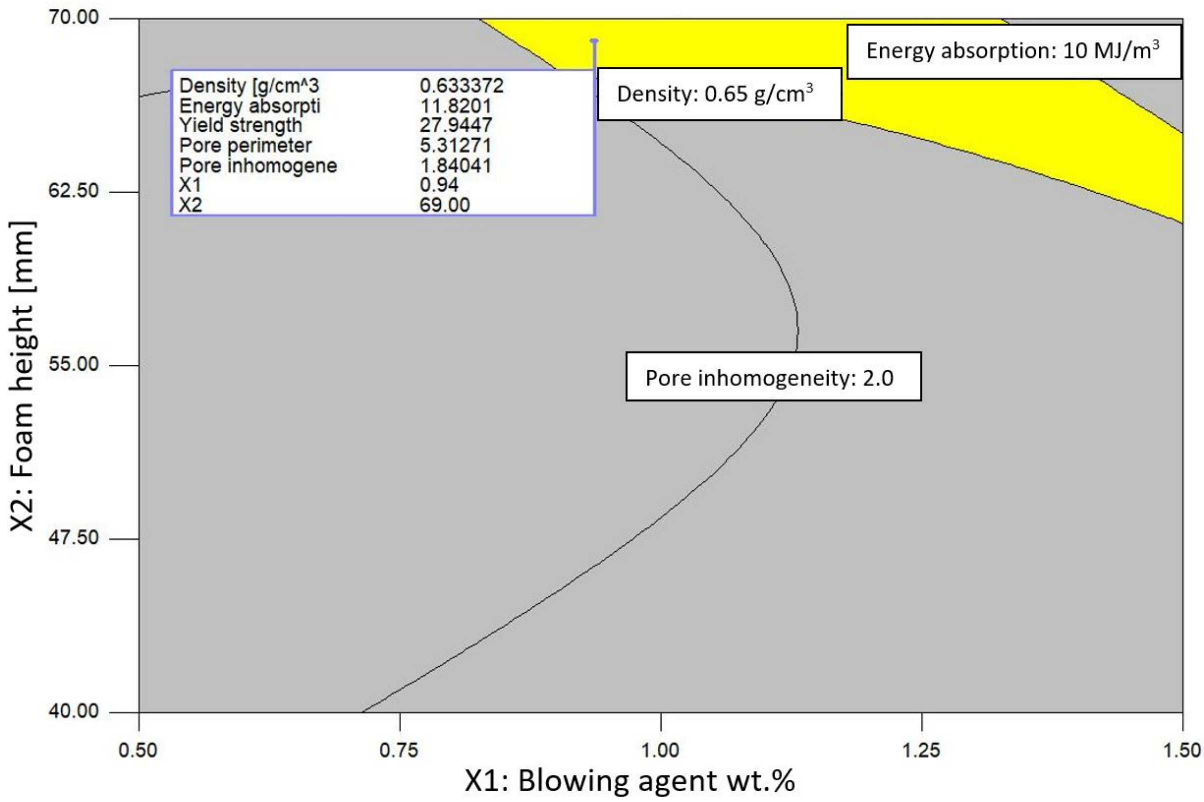

Figure 10. Graphical optimization of the process parameters for cost-effective metal foam production from machining chip waste.

4. Conclusions

Response surface methodology was used in this research to derive mathematical models that can describe the complex influence of production process parameters on metal foam properties. Using this approach, a cost-effective and environmentally friendly method for the production of aluminum waste-based metal foams was successfully described and optimized. The following conclusions can be derived:

(1) The production parameters used in the experimental plan were appropriately selected, and all 17 metal foams specimens were successfully produced, where plateau stress, energy absorption, and yield strength were in ranges from 21.8 MPa to 62.3 MPa, 10.9 MJ/m^3 to 31.3 MJ/m^3, and 14.4 MPa to 64.3 MPa, respectively. The obtained pore perimeter and pore inhomogeneity for all specimens were in the ranges of 3.2 to 7.4 mm and 1.4 to 4.8 mm, respectively.

(2) Energy absorption and yield strength generally increased with the reduction in the height of the metal foams due to the direct link with the metal foam density. For samples foamed with 0.5 and 1 (wt%) TiH_2 on 40 mm, 590 °C was more desirable than 610 °C for achieving higher energy absorption. However, for samples foamed at 70 mm when 1 or 1.5 (wt%) of TiH_2 was used, a significant increase in energy absorption was observed when 610 °C temperature was used instead of 590 °C.

(3) Three-dimensional optical profilometry was used to additionally evaluate the obtained metal foam quality. According to 3D scanning, the foam cell walls were quite homogeneous without any significant cracks. Pores were homogeneously dispersed across the metal foam cross-section, and the cell wall thickness was uniform for all created pores. Regression analysis was used to statistically analyze and describe the metal foam inhomogeneity.

(4) In accordance with the obtained mathematical models, the foam pore inhomogeneity increased with a higher amount of blowing agent at a 610 °C foaming temperature.

This was probably due to the lower semisolid slurry viscosity and higher amount of the blowing agent, which caused some pores to coagulate or to grow rapidly owing to the increased blowing gas pressure. This indicates that pore homogeneity can be reduced if both 1.5 (wt%) of the blowing agent and a 610 °C foaming temperature are selected.

(5) Foaming parameters also influence the pore perimeter. It seems that the foam pore perimeter increases with a lower amount of the blowing agent. The foam pore perimeter was highest with 0.5 (wt%) of the blowing agent and a 610 °C foaming temperature. It seems that at a 610 °C foaming temperature, foam pores increase with the decrease in the amount of the blowing agent for all foaming heights.

(6) Metal foam optimization, based on derived mathematical models, can be easily performed, but optimization criteria are directly connected with the possible application of the metal foams. In the optimization example provided in this research, the metal foam would have density, energy absorption, yield strength, pore diameter, and pore inhomogeneity values of 0.63 g/cm^3, 11.82 MJ/m^3, 27.9 MPa, 5.3 mm, and 1.84, respectively. This should be achieved if metal foam with 0.94 (wt%) of the blowing agent is foamed at 590 °C until a 69 mm height is reached.

Overall, according to the results presented in this research, it seems that quality closed-cell aluminum metal foams can be produced directly from machining chips. Compressive test and pore inhomogeneity analysis showed that the produced metal foams have characteristics comparable to some commercialized metal foams. The described process provides technology for both aluminum machining chip recycling and the production of cost-effective metal foams with the potential for commercialization of the process. Therefore, both economic and environmental benefits were achieved in this research.

Author Contributions: Conceptualization, J.K. and B.L.; methodology, J.K. and B.L.; software, K.G.; validation, K.G. and S.J.; formal analysis, J.K.; investigation, J.K. and B.L.; resources, K.G.; data curation, S.J. and K.G.; writing—original draft preparation, J.K.; writing—review and editing, B.L.; visualization, S.J.; supervision, S.J.; funding acquisition, S.J. and B.L. All authors have read and agreed to the published version of the manuscript.

Funding: This work was financially supported by the Croatian Science Foundation through the project Recycling of aluminum alloys in the solid and semisolid state (IP-2020-02-8284).

Data Availability Statement: Not applicable.

Conflicts of Interest: The authors declare no conflict of interest.

Abbreviations

ANOVA: variance analysis; RA: regression analysis; $Rp_{0.2}$: yield strength; S.D.: standard deviation.

References

1. Ashby, M.M.; Evans, A.; Fleck, N.A.; Hutchinson, J.W.; Wadley, H.N.G.; Gibson, L.J. *Metal Foams: A Design Guide*; Butterworth-Heinemann: Woburn, UK, 2002.
2. Wang, E.; Sun, G.; Zheng, G.; Li, Q. On multiaxial failure behavior of closed-cell aluminum foams under medium strain rates. *Thin Walled Struct.* **2021**, *160*, 107278. [CrossRef]
3. Ali, H.; Gábora, A.; Naeem, M.M.; Kalácska, G.; Mankovits, T. Effect of the manufacturing parameters on the pore size and porosity of closed-cell hybrid aluminum foams. *Int. Rev. Appl. Sci. Eng.* **2021**, *12*, 230. [CrossRef]
4. Commercial applications of metal foams: Their properties and production. *Materials* **2016**, *9*, 85. [CrossRef]
5. Wang, E.; Sun, G.; Zheng, G.; Li, Q. Characterization of initial and subsequent yield behaviors of closed-cell aluminum foams under multiaxial loadings. *Compos. Part B Eng.* **2020**, *202*, 108247. [CrossRef]
6. Martín, E.P. Microstructural parameters affecting the compressive response of closed-cell aluminum foams. *Mech. Adv. Mater. Struct.* **2021**, *28*, 1–20. [CrossRef]
7. Grilec, K.; Bunjan, I.; Jakovljević, S. The influence of applied force on aluminium foams energy absorption. *Teh. Vjesn.* **2021**, *28*, 1388–1394. [CrossRef]

8. Banhart, J. Production of Metal Foams. In *Beaumont PWR*; Zweben, C.H., Ed.; Comprehensive Composite Materials II; Elsevier: Amsterdam, The Netherlands, 2018; pp. 347–363.
9. Duarte, I.; Vesenjak, M.; Krstulović-Opara, L.; Anžel, I.; Ferreira, J.M. Manufacturing and bending behaviour of in situ foam-filled aluminium alloy tubes. *Mater. Des.* **2015**, *66*, 532–544. [CrossRef]
10. Baumgärtner, F.; Duarte, I.; Banhart, J. Industrialization of Powder Compact Toaming Process. *Adv. Eng. Mater.* **2000**, *2*, 168–174. [CrossRef]
11. Ghaleh, M.M.; Ehsani, N.; Baharvandi, H.R. High-Porosity Closed-Cell Aluminum Foams Produced by Melting Method Without Stabilizer Particles. *Int. J. Met.* **2021**, *15*, 899–905. [CrossRef]
12. Matijašević-Lux, B. *Characterisation and Optimisation of Blowing Agent for Making Improved Metal Foams*; Technische Universität Berlin: Berlin, Germany, 2006; p. 108.
13. Madhu, H.H.; Kailas, S.V. Fabrication of localised aluminium foam by a novel polymeric blowing agent. *Mater. Charact.* **2018**, *142*, 340–351. [CrossRef]
14. Rajak, D.D.; Kumaraswamidhas, L.L.; Das, S. On the influence of porosity and pore size on AlSi17 alloy foam using artificial neural network. *Ciencia. Tecnol. Mater.* **2017**, *29*, 14–21. [CrossRef]
15. Banhart, J.; Baumeister, J. Weber M Powder Metallurgical Technology for the Production of Metallic Foams Experimental procedure Preparation of metal foams. *Proc. Eur. Conf. Adv. PM Mater.* **1995**, 201–208.
16. Shiomi, M.; Imagama, S.; Osakada, K.; Matsumoto, R. Fabrication of aluminium foams from powder by hot extrusion and foaming. *J. Mater. Process. Technol.* **2010**, *210*, 1203–1208. [CrossRef]
17. Papantoniou, I.I.; Pantelis, D.D.; Manolakos, D.E. Powder metallurgy route aluminium foams: A study of the effect of powder morphology, compaction pressure and foaming temperature on the porous structure. *Procedia. Struct. Integr.* **2018**, *10*, 243–248. [CrossRef]
18. Stacey, M. *Aluminium Recyclability and Recycling*; Cwningen Press: Llundain, UK, 2015.
19. Kumar, N.; Bharti, A. Review on Powder Metallurgy: A Novel Technique for Recycling and Foaming of Aluminium-Based Materials. *Powder Met. Met. Ceram.* **2021**, *60*, 52–59. [CrossRef]
20. Duflou, J.J.; Tekkaya, A.A.; Haase, M.; Welo, T.; Vanmeensel, K.; Kellens, K.; Dewulf, W.; Paraskevas, D. Environmental assessment of solid state recycling routes for aluminium alloys: Can solid state processes significantly reduce the environmental impact of aluminium recycling? *CIRP Ann. Manuf. Technol.* **2015**, *64*, 37–40. [CrossRef]
21. Gronostajski, J.; Marciniak, H.; Matuszak, A. New methods of aluminium and aluminium-alloy chips recycling. *J. Mater. Process. Technol.* **2000**, *106*, 34–39. [CrossRef]
22. Hangai, Y.; Kobayashi, R.; Suzuki, R.; Matsubara, M.; Yoshikawa, N. Aluminum foam-filled steel tube fabricated from aluminum burrs of die-castings by friction stir back extrusion. *Metals* **2019**, *9*, 124. [CrossRef]
23. Tsuda, S.; Kobashi, M.; Kanetake, N. Producing technology of aluminum foam from machined chip waste. *Mater. Trans.* **2006**, *47*, 2125–2130. [CrossRef]
24. Kanetake, N.; Kobashi, M.; Tsuda, S. Foaming behavior of aluminum precursor produced from machined chip waste. *Adv. Eng. Mater.* **2008**, *10*, 840–844. [CrossRef]
25. Wang, H.; Zhu, D.D.; Hou, S.; Yang, D.; Nieh, T.; Lu, Z. Cellular structure and energy absorption of Al–Cu alloy foams fabricated via a two-step foaming method. *Mater. Des.* **2020**, *196*, 1–8. [CrossRef]
26. Raj, R.R.; Daniel, B.S.S. Prediction of compressive properties of closed-cell aluminum foam using artificial neural network. *Comput. Mater. Sci.* **2008**, *43*, 767–773. [CrossRef]
27. Lela, B.; Krolo, J.; Grgić, K.; Sonja, J.; Dumanić, I. *Production of Closed Cell Foams from the Aluminium Chip Waste*; Croatian society for mechanical technologies: Split, Croatia, 2021; pp. 95–100.
28. Dumanić, I.; Krolo, J.; Lela, B.; Jozić, S. Thermomechanical treatment of A380 aluminum alloy for globular thixo feedstock. *Materwiss Werksttech* **2020**, *51*, 1047–1057. [CrossRef]